

## Synthesis, characterization, and performance of oligothiophene cyanoacrylic acid derivatives for solar cell applications



H. Al-Dmour<sup>1</sup>, Salah Al-Trawneh<sup>2</sup>, Samir Al-Taweel<sup>2,\*</sup>

<sup>1</sup>Department of Physics, Faculty of Science, Mu'tah University, Mu'tah, Jordan

<sup>2</sup>Department of Chemistry, Faculty of Science, Mu'tah University, Mu'tah, Jordan

### ARTICLE INFO

#### Article history:

Received 2 November 2020

Received in revised form

11 February 2021

Accepted 3 March 2021

#### Keywords:

Oligothiophene cyanoacrylic acid

Dye sensitizers

J-V characteristic

Synthesis

Nc-TiO<sub>2</sub> semiconductor

### ABSTRACT

New dye sensitizers based on an oligothiophene cyanoacrylic acid derivative were synthesized and characterized for solar cell applications. The structures of the new dyes prepared as sensitizers based on oligothiophenes, namely 5,5''-di-2-cyanoacrylic acid [2,2':5',2''-terthiophene] (dye1), [2,2':5',2''-terthiophene]-5-cyanoacrylic acid (dye2), and [2,2':5',2''':5'',2''''-quaterthiophene]-5-cyanoacrylic acid (dye3) were confirmed by elemental analysis, mass spectrometry, and <sup>1</sup>H-NMR spectral data. The P3HT/dye2/nc-TiO<sub>2</sub> solar cell produced the highest efficiency of 0.05% with an open circuit voltage of 0.65V compared to dyes 1 and 3 solar cells. That may have been attributed to the dyes' molecular structure, which had different chain lengths and numbers of groups of cyanoacrylic connected to the dyes' thiophene moiety. The dark current suppressed in the P3HT/dye2/nc-TiO<sub>2</sub> solar cells indicated the formation of the charge blocking layer, which produced an enhanced open-circuit voltage accompanied by a high onset voltage.

© 2021 The Authors. Published by IASE. This is an open access article under the CC BY-NC-ND license (<http://creativecommons.org/licenses/by-nc-nd/4.0/>).

### 1. Introduction

Hybrid photovoltaic cells, which are based on junctions between inorganic Nano-crystalline materials, hole transport layers, and organic dyes, so-called dye-sensitized solar cells (DSSCs) have attracted great attention. DSSCs have the potential for low-cost fabrication and ease of production, which makes them good candidates for commercialization (Baxter, 2012). Zinc porphyrin sensitizer SM371 with carboxylate ligand provides PSEs of 12.5-13.0% when employing a Co (II/III) redox system as an electrolyte (Yella et al., 2011) and efficiencies of 15% perovskite solid-state DSSC (Burschka et al., 2013). Ru complexes with carboxylate bipyridine ligands were first used to sensitize TiO<sub>2</sub> single crystals (O'Regan and Grätzel, 1991).

Nazeeruddin et al. (1993) prepared a series of mononuclear Ru-complexes, a thiocyanate derivative, cis-(SCN<sub>2</sub>) bis (2, 2'-bipyridyl-4,4'-dicarboxylate) ruthenium (II), coded as N3, exhibited 10% efficiency (Nazeeruddin et al., 1993). Metal-free

organic photosensitizers have significant advantages over noble Ru-complex sensitizers due to their low production cost, synthetic facial methodology for diverse molecular structures, and higher extinction coefficients (Selopal et al., 2016). Despite these properties, to date, the performance of DSSCs based on metal-free dyes has lagged behind those with metal-organic dyes as a result of their high recombination losses and lower open-circuit voltage (Voc). A few recent metal-free oligothiophene-based dyes in combination with (I<sup>-</sup>/I<sub>3</sub><sup>-</sup>) redox systems showed this approach's potential, as these systems have excellent efficiencies of up to 9.8% (Fig. 1).

For efficient electron injection into the anodes, the dye structure has donor-to-acceptor (D-A) moieties bridged by -conjugated thiophene systems such as oligothiophenes, thienylene vinylenes, thienothiophenes, and dithienothiophenes as  $\pi$  donors and a cyanoacrylic acid moiety as an electrophilic/anchoring acceptor group. The most prominent class of metal-free sensitizers for DSSCs was reviewed by Bauerle in *Angewandte Chemie* (Bauerle et al., 2009) and Hagfeldt in *Chemical Reviews* (Hagfeldt et al., 2010). In the present investigation, we prepared new dyes as sensitizers based on oligothiophenes, namely 5,5''-di-2-cyanoacrylic acid [2,2':5',2''-terthiophene] (dye1), 5-[2,2':5',2''-terthiophene]-2-cyanoacrylic acid (dye 2), and 5-[2,2':5',2''':5'',2''''-quaterthiophene]-2-cyanoacrylic acid (dye 3) (Fig. 2).

\* Corresponding Author.

Email Address: [s\\_altaweel@mutah.edu.jo](mailto:s_altaweel@mutah.edu.jo) (S. Al-Taweel)

<https://doi.org/10.21833/ijaas.2021.06.015>

Corresponding author's ORCID profile:

<https://orcid.org/0000-0002-0250-4187>

2313-626X/© 2021 The Authors. Published by IASE.

This is an open access article under the CC BY-NC-ND license

(<http://creativecommons.org/licenses/by-nc-nd/4.0/>)

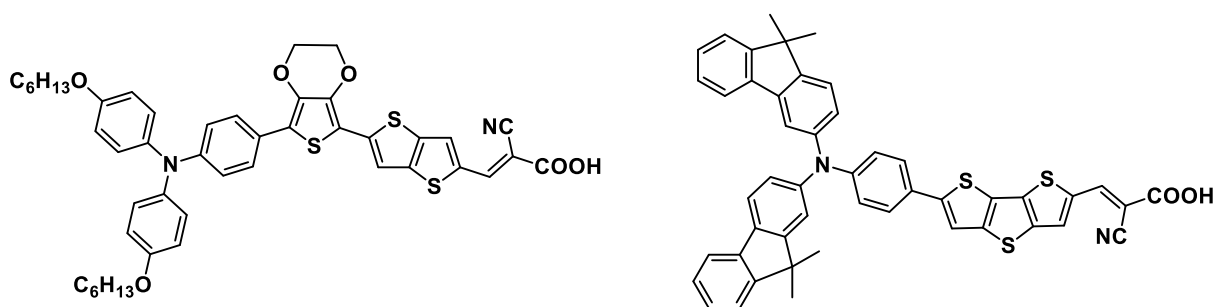


Fig. 1: The chemical structure of metal-free oligothiophene-based dyes

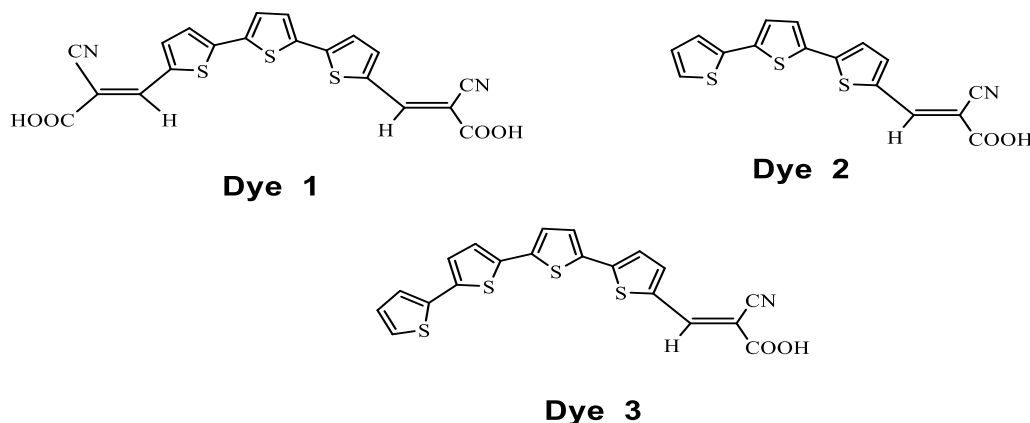


Fig. 2: The chemical structures of dyes 1, 2 and 3

The structure contains cyanoacrylic acid as an electrophilic acceptor moiety related to a  $\pi$ -conjugated  $\alpha$ -terthiophene and  $\alpha$ -quaterthiophene. From a practical perspective, it is critical to use non-volatile and solvent-free electrolytes as hole transport materials, poly(3-hexylthiophene) as iodine-free and non-volatile electrolytes is employed to investigate organic/inorganic solar cell characteristics.

## 2. Experimental method

### 2.1. Chemistry

N-butyllithium, N-formylpiperidine, lithium hydroxide, palladium (II) acetate, and cesium fluoride were purchased from Sigma-Aldrich. Thiophene and N-bromosuccinimide were purchased from Janssen. 2-Mercaptoethyl acetate, calcium carbonate, potassium carbonate, sodium sulfate, dimethyl formamide, 2-bromo-5-thiophenecarboxaldehyde, Tetrahydrofuran, magnesium sulfate, and sodium hydroxide were purchased from Acros. Bromine, cuprous iodide, and Phosphorus oxychloride were purchased from Fluka. Silica gel for column chromatography was purchased from Macherey-Nagel and Co. GmbH (Germany). Tetrahydrofuran was dried over sodium metal/benzophenone and then distilled and collected under a nitrogen atmosphere. Dichloromethane was dried over  $P_2O_5$ . Melting points were determined on a scientific melting point apparatus in open capillary tubes.  $^1H$ -NMR and  $^{13}C$ -NMR spectra were recorded on a 400MHz spectrometer (Bruker Avance III 400MHz) (Al-

Yarmouk University) with TMS as the internal standard for  $CDCl_3$  solution. Chemical shifts are expressed in  $\delta$  units. High-resolution mass spectra (HRMS) were measured by electrospray ionization (ESI) on a Bruker APEX-IV instrument (University of Jordan). The samples were dissolved in chloroform, diluted in spray solution (methanol/chloroform), and infused using a spring pump with a flow rate of  $2\mu L/min$ . Elemental analysis (CHN) was determined by EA.96-mth (University of Jordan).

Synthesis of 5,5''-bis-2-cyanoacrylic acid [2, 2':5, 2''-terthiophene] (dye1).

Acetonitrile (5ml) solution with 5,5''-diformyl-[2,2':5,2''-terthiophene] (6) (100mg, 0.33mmole), cyanoacetic acid (57mg, 0.66mmole), and piperidine (0.1g) was refluxed for 24h under a nitrogen atmosphere. The reaction mixture was added to petroleum ether (15ml) and HCl (15ml, 0.1M). A dark red precipitate formed, which was filtered to yield dye 1 (100mg, 80%) with m.p.=255°C (decomposition).  $^1H$ NMR ( $DMSO-d_6$ , 400MHz): ppm,  $\delta$ =8.85 (s, 1H), 7.95 (d, 1H,  $J=4$ Hz), 7.68 (d, 2H,  $J=4$ Hz), and 7.67 (s, 2H).  $^{13}C$ -NMR: ( $DMSO-d_6/100$ MHz): ppm,  $\delta$ =126.6, 128.8, 136.9, 139.7, 142.4, 144.7, and 184.5. UV-VS was conducted ( $\lambda=400$ nm,  $CHCl_3$ ).

Synthesis of 5, 5''-diformyl- 2, 2':5', 2''-terthiophene (6).

$POCl_3$  (16 mmol, 2.4g) was added dropwise into a 50ml round-bottomed flask containing DMF (16mmol, 1.17g) and dry  $CH_2Cl_2$  (5ml) at 0°C and stirred. The mixture was removed from an ice bath and warmed at  $\sim 40^\circ C$  until a clear pale-yellow solution was obtained. Vilsmeier reagent was then added dropwise into a flask containing a solution of

2, 2':5', 2''-terthiophene (4) (0.2g, 0.8mmol) in 5ml of dry CH<sub>2</sub>Cl<sub>2</sub> at 0°C. The color changed from yellow to red with small crystals and started to precipitate. After refluxing for 24h, the CH<sub>2</sub>Cl<sub>2</sub> evaporated. Cold aqueous NaOH (1M) was then added, and the mixture was heated in a steam bath for 2h. The mixture was filtered and washed with water, and drying produced a red powder. Column chromatography (hexane/CH<sub>2</sub>Cl<sub>2</sub>) (1/1) was conducted to produce 0.2g of red solid with m.p.=215°C (yield~90%). <sup>1</sup>H-NMR (DMSO-d<sub>6</sub>, 400MHz): ppm, δ=9.91 (s, 2H), 8.02 (d, 2H, J=4Hz), 7.66 (s, 2H), and 7.62 (d, 2H, J=4Hz). <sup>13</sup>C-NMR (DMSO-d<sub>6</sub>/100MHz): ppm, δ=184.48, 144.71, 142.40, 139.66, 136.87, 128.84, and 126.59.

Synthesis of [2,2':5',2''-terthiophene] 5-cyanoacrylic acid (dye 2).

Acetonitrile (5ml) solution with 5-formyl- [2, 2':5',2''-5'']-terthiophene (5) (120mg, 0.43mmole), cyanoacetic acid (80mg, 0.86mmole), and piperidine (0.1g) were refluxed for 24h under a nitrogen atmosphere. The reaction mixture was added to petroleum ether (15ml) and HCl (15ml, 0.1M). A dark red precipitate formed that was filtered to yield 110mg, 80% with m.p.=255°C. <sup>1</sup>H-NMR (DMSO-d<sub>6</sub>, 400MHz), ppm: δ=8.84 (s, 1H), 7.975 (d, 1H, J=4Hz), 7.60 (m, 3H), 7.45 (d, 2H, J=4Hz), 7.39 (d, 1H, J=4Hz), and 7.13 (dd, 1H, J=4Hz). <sup>13</sup>C-NMR (DMSO-d<sub>6</sub>/100MHz), ppm: δ=165.65, 163.55, 145.98, 144.88, 141.30, 138.35, 135.44, 134.06, 133.43, 128.64, 128.07, 126.66, 125.49, 125.21, 125.05, 116.67, and 115.66. UV-VS was conducted. (λ=440 nm, CHCl<sub>3</sub>).

Synthesis of 5-formyl- [2, 2':5', 2'']-terthiophene (5).

DMF (0.25ml, 3mmol, 0.24g) and dry CH<sub>2</sub>Cl<sub>2</sub> (5ml) at 0°C, 0.28ml POCl<sub>3</sub> (3mmol, 0.46) were added dropwise into a capped Erlenmeyer flask with stirring. The mixture was removed from an ice bath and warmed to ~40°C until a clear pale yellow solution was obtained. Vilsmeier reagent was then added dropwise into a flask containing a solution of 2, 2':5', 2''-terthiophene (0.5g, 2mmol) in 5ml of dry CH<sub>2</sub>Cl<sub>2</sub> at 0°C. The color changed from yellow to red and small crystals started to precipitate. After standing for 24h at room temperature, the CH<sub>2</sub>Cl<sub>2</sub> evaporated. Cold aqueous NaOH (1M) was then added, and the mixture was heated in a steam bath for 2h. The mixture was filtered and washed with water, and drying produced a yellow powder. Column

chromatography (hexane/dichloromethane) 1/1) was conducted to produce a yellow solid, 0.4g with m.p.=137°C (yield~72%). <sup>1</sup>H-NMR (CDCl<sub>3</sub>-d<sub>1</sub>, 400MHz), ppm: δ=9.87 (s, 1H), 7.68 (d, 1H, J=4Hz), 7.30 (m, 2H), 7.24 (m, 2H), 7.145 (d, 1H, J=4Hz), and 7.067 (dd, 2H, J=5Hz).

Synthesis of [5,2':5',2'':5'',2''']-quaterthiophene] 5-cyanoacrylic acid (dye 3).

Acetonitrile (5ml) solution with 5-formyl- [5,2':5',2'':5'',2''']-quaterthiophene (8) (45mg, 0.11mmole), cyanoacetic acid (20mg, 0.22mmole), and piperidine (0.1g) were refluxed for 24h under a

nitrogen atmosphere. The reaction mixture was added to petroleum ether (15ml) and HCl (15ml, 0.1M). A dark red precipitate formed that was filtered to produce 40 mg, 90% yield, with m.p.=230°C. <sup>1</sup>H-NMR (DMSO-d<sub>6</sub>/400MHz), ppm: δ=7.11 (dd, J=4.8Hz), 7.31 (d, J=4.0Hz), 7.37 (dd, J=3.6Hz, J=1.2Hz), 7.41 (m), 7.55 (dd), 7.60 (dd), 7.98 (dd, J=4.0Hz), and 8.48 (s). UV-VS was then conducted (λ=440nm, CHCl<sub>3</sub>).

Synthesis of 5-formyl- [5,2':5',2'':5'',2''']-quaterthiophene (8).

Freshly dried THF (10ml) was added to a mixture of 2-bromo-5-thiophene carboxaldehyde (7) (0.23g, 1.2mmol) and 5-trimethylstannyl- [2,2':5',2'']-terthiophene (7) (0.53g, 1.3mmole). Pd (Ph<sub>3</sub>P)<sub>2</sub>Cl<sub>2</sub> (0.042g, 0.06mmol) was added to this solution under nitrogen. The reaction was refluxed for 24h and then cooled. The THF was evaporated, water (20ml) was then added, and the reaction mixture was extracted with diethyl ether (20mlx3). The combined ethereal extracts were washed with water (30ml) and then brine (30ml). The organic layer was dried over anhydrous MgSO<sub>4</sub> and the ether evaporated, followed by recrystallization from hexane to produce 0.3g, with a 68% yield of orange powder with m.p.=209-211°C. <sup>1</sup>H-NMR (200 MHz, DMSO-d<sub>6</sub>): ppm: δ=10.00 (s, 1H, CHO proton), 7.2-8.2 (m, 9H), and MS (EI). The m/e intensity was 358 (100) M, 359 (27) M+1, 330 (5), 313 (2), 285 (15), 272 (3), 248 (20), 222 (7), 203 (5), 179 (6), 165 (8), 143 (11), 127 (7), and 69 (12). For C<sub>17</sub>H<sub>10</sub>O: C, 56.99 and H, 2.82, producing C 57.13 and H 2.94.

Synthesis of 5-trimethylstannyl- [2, 2':5', 2'']-terthiophene (7).

Hexane was added to a solution of 2, 2':5', 2''-terthiophene (4) (1.5g, 6.1mmol) in dry ether (15 ml) at -30°C, n-butyl lithium (2.42ml, 6.1mmol) for 10 min with continuous stirring, and trimethylstannyl chloride (1.22g, 6.1mmole) was added in one portion. Stirring continued for 30 min at room temperature. The solvent was removed under reduced pressure. An oily residue was extracted with 3x 15ml of hexane. The hexane was removed to produce 2.0 g of yellow crystals with an 80% yield and m.p.=52-54°C. This compound was used without further purification. <sup>1</sup>H-NMR (CDCl<sub>3</sub>, 200 MHz) δ=6.85-7.30 (m, 9H), and 0.45 (s, 9H).

## 2.2. Fabrication of the polymer solar cells

In this investigation, the solar cells were fabricated with SnO<sub>2</sub> to produce F/nc-TiO<sub>2</sub>/dye/P3HT/AU solar cells. Before fabricating the solar cells, SnO<sub>2</sub>: F was cleaned using Decon 90 and rinsed in ultrapure water, hot water, and ethanol, and dried for 5 min under a nitrogen stream. Using the doctor blade technique (Al-Dmour, 2014), the electron transporting nc-TiO<sub>2</sub> layers were coated onto SnO<sub>2</sub>: Felectrodes from a paste of nc-TiO<sub>2</sub> Solaronix. After drying at 100°C for 15 min, the film was heated to 450°C for 30min and then slowly cooled to room temperature. The nc-TiO<sub>2</sub> was typically 2μm thick as determined by a scanning

electronic microscope. The dye/nc-TiO<sub>2</sub>/SnO<sub>2</sub>: F film was prepared by soaking SnO<sub>2</sub>/nc-TiO<sub>2</sub> electrodes in a dye solution at room temperature for 12h to absorb the dye. In the second step, the substrate was removed, rinsed in ethanol, and dried under a nitrogen flow for 3m. Hole-transporting P3HT was prepared by dissolving 0.03g of P3HT in 2ml of chloroform (Sigma-Aldrich), yielding a concentration of 1% w/w. The P3HT solution was spin-coated onto the SnO<sub>2</sub>: F/nc-TiO<sub>2</sub>/dye at a spin speed of 1000 rpm for 60 a. AU electrodes were vacuum deposited on top of the P3HT at pressures below 3×10<sup>-6</sup>Torr to obtain an active area of 0.03cm<sup>2</sup> (Fig. 3).

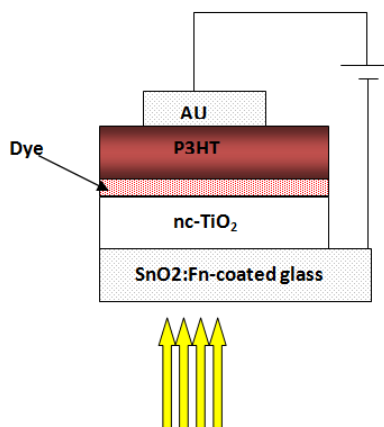


Fig. 3: Schematic diagram of the AU/P3HT/dye/nc-TiO<sub>2</sub>/SnO<sub>2</sub>: F solar cells

Current-voltage (I-V) characteristics were obtained using a Keithley model 307 source

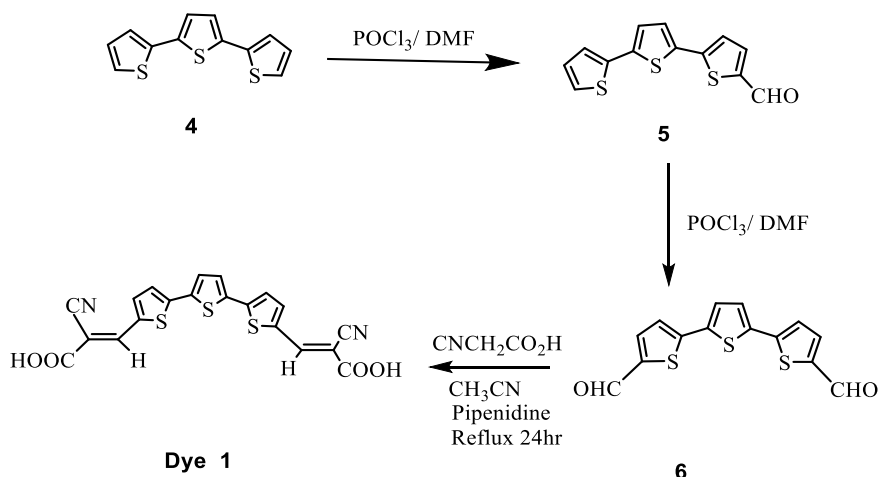


Fig. 4: Preparation of 5, 5''-bis-2-cyanoacrylic acid [2, 2':5', 2''-terthiophene]

[2, 2':5', 2''-terthiophene]-5-cyanoacrylic acid, dye 2 was prepared by reaction of 5-formyl-2, 2':5', 2''-terthiophene (5) with cyanoacetic acid in acetonitrile using piperidine as base to afford dark red solid in 87%, (Fig. 5). 5-Formyl- 2, 2':5', 2''-terthiophene (5)

measurement unit. A xenon lamp was used to illuminate the devices through the transparent electrodes, with the light (incident power of 100mW/cm<sup>2</sup>) constrained by an aperture to fall on areas coinciding with one of the top gold electrodes.

### 3. Results and discussion

#### 3.1. Synthesis of dye sensitizers

The synthetic approaches to dyes involve Vilsmeier formylation, Stille coupling (Stille, 1986), and Knoevenagel condensation (Knoevenagel, 1894) are presented in Figs. 4, 5, 6. The chemical synthesis of dye (1) involves the reaction of 5,5''-diformyl- 2, 2':5', 2''-terthiophene (6) with two moles of cyanoacetic acid in acetonitrile using piperidine as a base to afford dark red solid in 90% as shown in Fig. 4. The synthesis of 5,5''-diformyl- 2, 2':5', 2''-terthiophene (6) directly from 2, 2':5', 2''-terthiophene (4) using two or three moles of DMF/POCl<sub>3</sub> was unsuccessful, the monoaldehyde was isolated as a major product with a small amount of the desired dialdehyde as evidence from <sup>1</sup>HNMR. However, the dialdehyde was produced by the reaction of 5-formyl- 2, 2':5', 2''-terthiophene (5) with fresh Vilsmeier reagent made of two moles of DMF/POCl<sub>3</sub> with only 35% yield. Finally, the dialdehyde was prepared in 95% yield by the reaction of 2, 2':5', 2''-terthiophene (4) with 20 mole excess of Vilsmeier reagent under reflux for 24 hours.

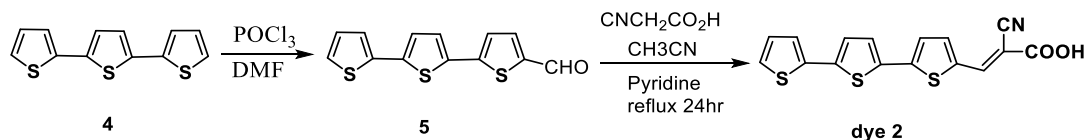


Fig. 5: Preparation of [2, 2':5', 2''-terthiophene] 5-cyanoacrylic acid, dye 2

For [2, 2':5, 2'':5'', 2'''-quaterthiophene] 5-cyanoacrylic acid, dye 3, it was prepared by the reaction of 5-formyl- [2, 2':5', 2'':5'', 2'''-quaterthiophene (8) with cyanoacrylic acid in acetonitrile using piperidine as base to afford dark red solid in 90% yield with m.p.=230C<sup>0</sup>. Formyl- [2,2': 5',2'':5'',2'''-quaterthiophene (8) was prepared via Stille coupling between 5-trimethylstannyl [2, 2': 5', 2'''-terthiophene (7) and 2-bromo-5-thiophene

carbaldehyde in the presence Pd(Ph<sub>3</sub>P)<sub>2</sub>Cl<sub>2</sub> as catalyst in 68% yield as orange powder with m.p.=209-211C<sup>0</sup>. While 5-trimethylstannyl [2, 2':5', 2'''-terthiophene (7) was prepared via lithiation of [2, 2':5', 2'''-terthiophene (4) in dry ether at -78°C using n-butyl lithium, followed by reaction with trimethyltin chloride, and used with no farther purification (Fig. 6).

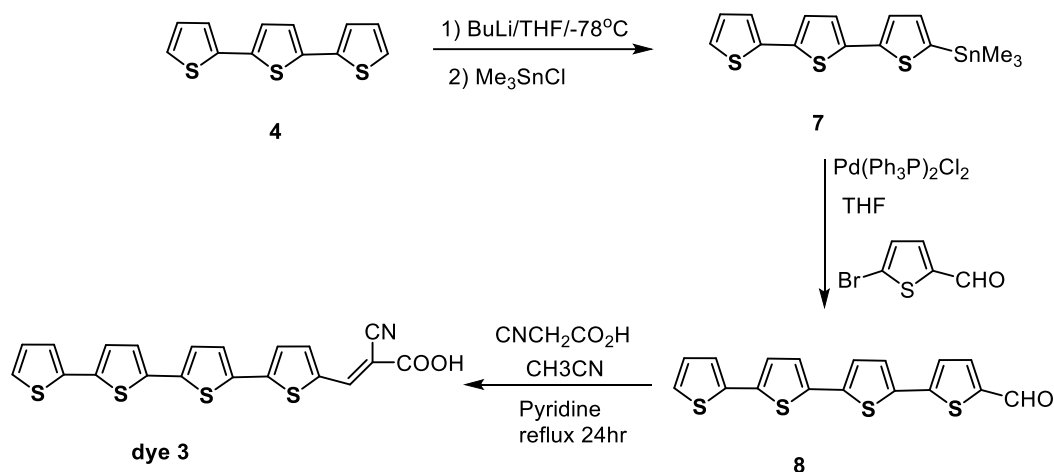


Fig. 6: Preparation of [2, 2':5', 2'':5'', 2'''quaterthiophene] 5-cyanoacrylic acid, dye 3

### 3.2. Optical properties

Fig. 7 shows the UV-VS absorption spectra of the SnO<sub>2</sub>: F/nc-TiO<sub>2</sub>/P3HT film and dyes 1, 2, and 3 inserted between the nc-TiO<sub>2</sub> and P3HT layers and compact TiO<sub>2</sub> layer. The films' light absorbance with dyes 2 and 3 was higher than the nc-TiO<sub>2</sub>/P3HT film in a range of 400nm to 600nm while dye 1 had higher absorbance in a range of 400nm to 500nm. This result indicated that the dyes' solar cells

enhanced the absorption of incident light and increased the efficiency observed in the nc-TiO<sub>2</sub>/dye/P3HT solar cells. Dye 2's absorbance was higher than the absorbance of dyes 1 and 3. It depended on the differences in the dyes' energy gaps and energy levels, which were related to the materials' structures. For the compact TiO<sub>2</sub> layer, the film has maximum absorbance which is related to the energy gap of TiO<sub>2</sub>.

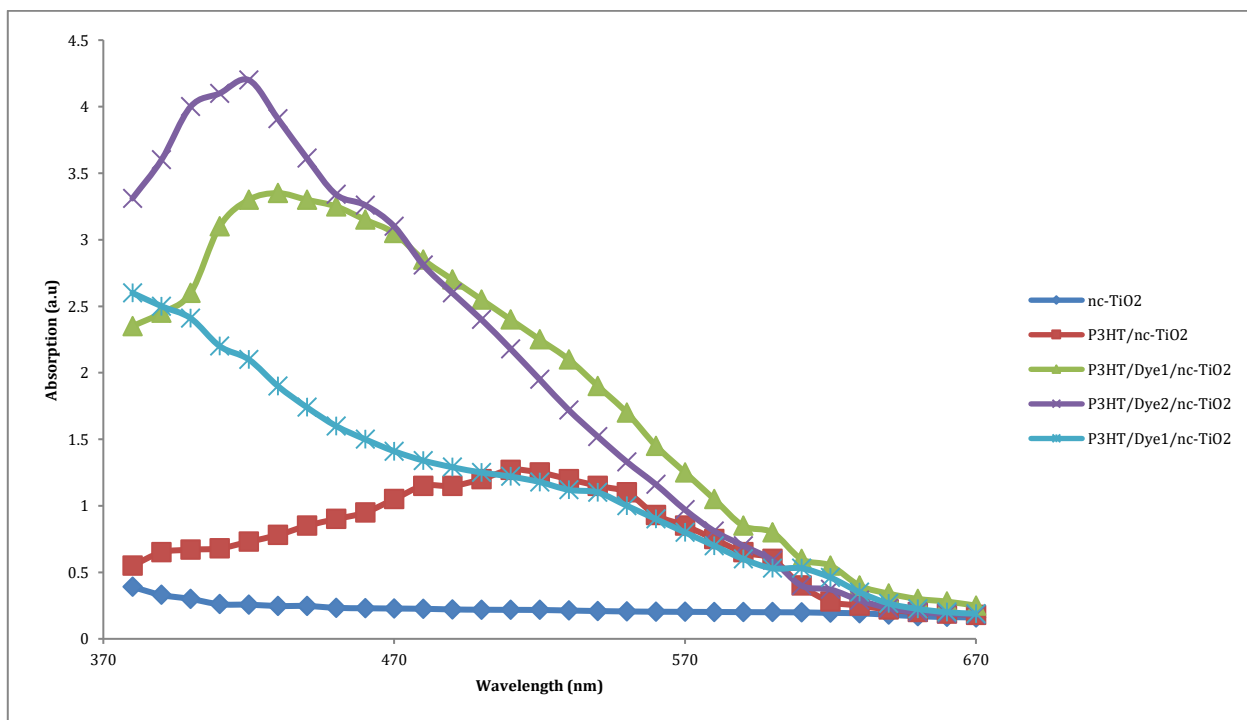


Fig. 7: UV-VS absorption spectra of the nc-TiO<sub>2</sub>/P3HT, nc-TiO<sub>2</sub>/dye1, nc-TiO<sub>2</sub>/dye2and nc-TiO<sub>2</sub>/dye3 thin films

### 3.3. Effect of dye structure on solar cells performance

The dye structure plays an important role in improving the efficiency of metal oxide-organic solar cells (Saleh et al., 2015) since the dye enhances charge separation that occurs at the interfaces between the holes and electron transport layers. Three solar cells were constructed using synthesized dye: Dyes 1, 2, and 3. These dyes were individually inserted between the nc-TiO<sub>2</sub> and P3HT films to modify the properties of interfacial areas between the films. The structures of the devices became SnO<sub>2</sub>: F/nc-TiO<sub>2</sub>/dye/P3HT solar cells. The main parameters of new solar cells were short circuit current density (J<sub>sc</sub>), open-circuit voltage (V<sub>oc</sub>), maximum output power (P<sub>max</sub>), fill factor (FF), and

power conversion efficiency (η<sub>e</sub>) extracted from the J-V curves. These properties are summarized in Table 1. The devices' J-V characteristics were measured under illumination (100mA/cm<sup>2</sup>=P<sub>i</sub>) as light power as shown in Fig. 8. The short circuit current density (J<sub>sc</sub>) increased from 0.11 mA/cm<sup>2</sup> in dye 1 to 0.16mA/cm<sup>2</sup> in dye 2 accompanied by an enhanced open-circuit voltage (V<sub>oc</sub>) from 0.40V to 0.65V. The fill factor (FF) and power conversion (η) values were calculated using Eqs. 1 and 2:

$$FF = \frac{P_{max}}{V_{oc} \cdot J_{sc}} \tag{1}$$

$$\eta = \frac{P_{max}}{P_i} \tag{2}$$

where P<sub>i</sub> stands for light intensity.

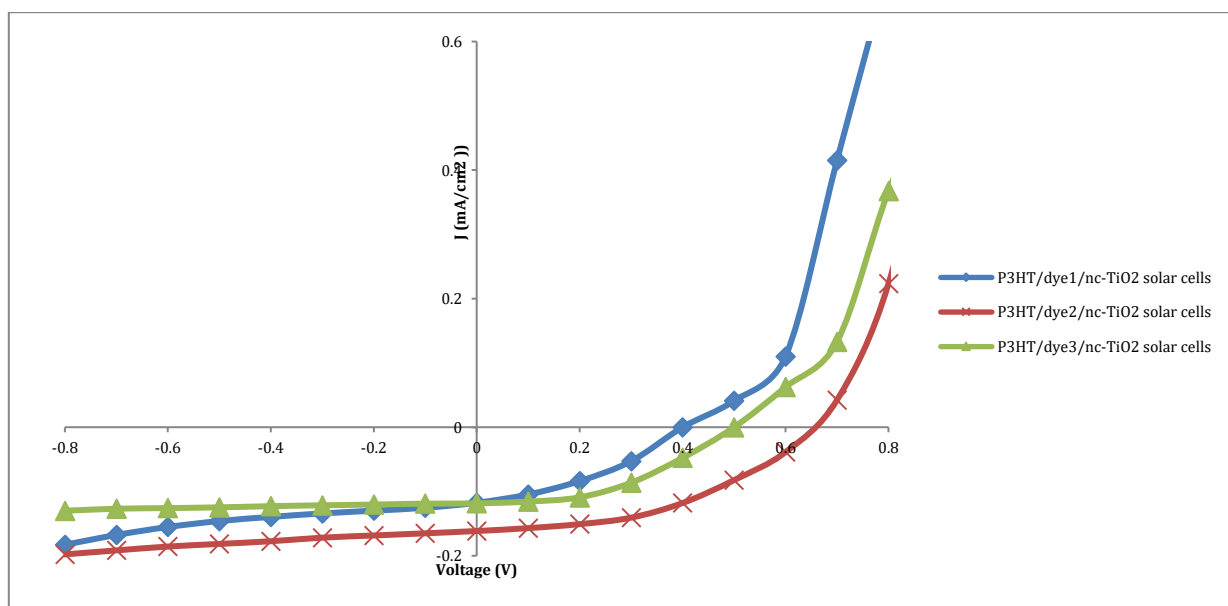


Fig. 8: J-V characteristics of the nc-TiO<sub>2</sub>/dye1/P3HT, nc-TiO<sub>2</sub>/dye2/P3HT and nc-TiO<sub>2</sub>/dye3 /P3HT solar cells under light illumination

In this study, the P3HT/dye2/nc-TiO<sub>2</sub> had the best solar cell performance. It produced a fill factor (FF) of 47% and a power conversion efficiency (η<sub>e</sub>) of 0.05%, which was twice as high as the other devices. The P3HT/dye3/nc-TiO<sub>2</sub> and P3HT/dye1/nc-TiO<sub>2</sub> solar cells had a power conversion efficiency of 0.03% and 0.02%, respectively, that was attributed to the lower response to the light falling on these solar cells. Dye 3's absorption curves demonstrated that it absorbed more light than the other dyes. Fig. 9 shows the current density vs voltage (J-V) of typical solar cells fabricated using the three different dyes under dark

conditions. The results showed that the rectification ratios ranged from 10 for dye 1 to 10<sup>4</sup> for dye 2 at ±1 V. As the forward bias voltage applied on the Au electrodes increased, the devices became conducting current at different voltage values. This value is called the onset forward conduction voltage, which decreased from 0.8V in dye 2's solar cells to 0.6 V dye 3's solar cells. Dye 1's solar cells did not show good diode behavior, with small rectifications less than 10. Dye 3's dark current increased more rapidly than the other devices.

Table 1 summarizes the photovoltaic output parameters of the solar cells studied in this work.

Table 1: Photovoltaic parameters of solar cells with different dyes

Parameters	P3HT/dye1/ nc- TiO2 solar cell	P3HT/dye2/ nc- TiO2 solar cell	P3HT/dye3 /nc- TiO2 solar cell
J <sub>sc</sub> (mA/cm <sup>2</sup> )	0.11	0.16	0.12
V <sub>oc</sub> (V)	0.40	0.65	0.50
η <sub>e</sub> %	0.02	0.05	0.03
FF %	34.0	48.0	43.0
Rectification Ratio	10	10000	1000
V <sub>onset</sub> (V)	0.55	0.80	0.60

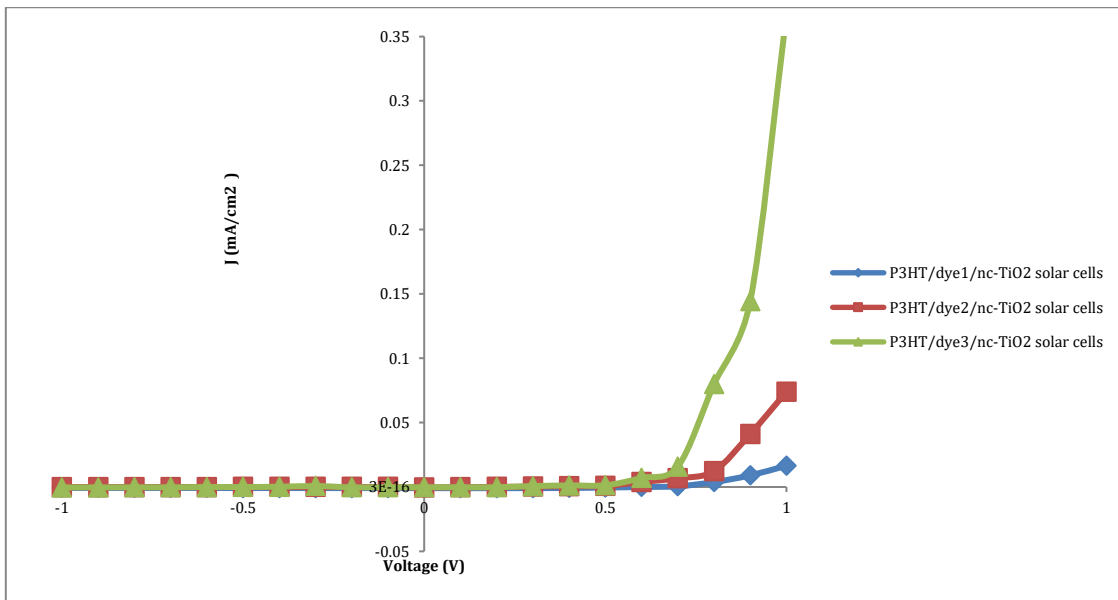


Fig. 9: J-V characteristics of the nc-TiO<sub>2</sub>/dye1/P3HT, nc-TiO<sub>2</sub>/dye2/P3HT and nc-TiO<sub>2</sub>/dye3 /P3HT solar cells under dark conditions

These data presented a relationship between the values of the onset voltage and dark current density with open circuit voltage. Similarly, the data demonstrated a relationship between the onset voltage values and dark current density with open circuit voltages. Similar to our results, Neil reported an increase in the onset voltage and a suppression of the dark current, accompanied by an enhancement of the open circuit voltage value (Li et al., 2009) Fig. 10 shows the equivalent circuit of organic/inorganic solar cells; the effect of the components is presented as R<sub>s</sub> and R<sub>sh</sub>.

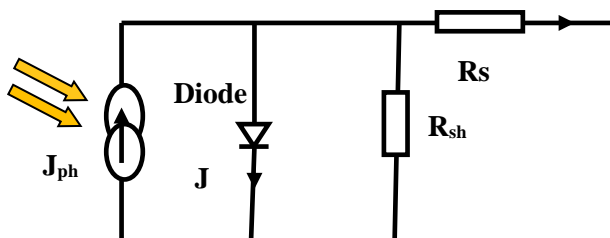


Fig. 10: Electric equivalent circuit of organic solar cells

In this circuit, the organic solar cells' net current density (J<sub>net</sub>) is expressed as (Li et al., 2009):

$$J = \frac{R_p}{R_{sh} + R_s} \left\{ J_s \left[ \exp\left(\frac{q(V - JR_s)}{nK_B T}\right) - 1 \right] + \frac{V}{R_{sh}} \right\} - J_{ph}(V) \quad (3)$$

where, V is the bias voltage, J<sub>ph</sub> is the photocurrent, K<sub>B</sub> is the Boltzmann constant, T is the temperature, J<sub>s</sub> is the reverse dark saturation current density, and n is the ideality factor. Using the equation, V=V<sub>oc</sub> was obtained when a shunt resistor was larger than the series resistance and J=0mA/cm<sup>2</sup>. The V<sub>oc</sub> is described by:

$$V_{oc} = \frac{nK_B T}{q} \ln \left( \frac{J_{ph}(V_{oc})}{J_s} + 1 - \frac{V_{oc}}{J_s R_{sh}} \right) \quad (4)$$

As indicated in Eq. 4, J<sub>s</sub> should be small to achieve a high open-circuit voltage. The V<sub>oc</sub> is proportional to the Ln value (J<sub>ph</sub>/J<sub>s</sub>) when J<sub>ph</sub> << J<sub>s</sub>. At these values,

the Voc is small. In general, the dark current is suppressed by adding electrons and/or hole-blocking layers at the interfacial layers (Wang et al., 2020). That effectively weakens surface recombination at the donor and acceptor surfaces and improves the efficiency of electronics devices. In our results, the P3HT/dye 2/nc-TiO<sub>2</sub> solar cells suppressed the dark current more than the other devices and behaved like a diode in the dark with high rectification. Consequently, dye 2's layer reduced the charge leakage at the interfaces and improved the photo-charge separation and transport, acting as a charge-blocking layer. That may have been due to dye 2's energy levels, which were suitable for the energy levels of P3HT and nc-TiO<sub>2</sub>. In principle, for efficient P3HT/dye/nc-TiO<sub>2</sub> solar cells, during the regeneration of the sensitizers, the holes should move faster than the recombination of the conduction band electrons with oxidized sensitizers. The dyes' highest occupied molecular orbital (HOMO) was below the hole transporters' energy bands so that the oxidized dyes formed after electron injection into nc-TiO<sub>2</sub>'s conduction band, which was effectively regenerated by accepting electrons from the hole transporters.

Dye 2 had high aggregation, demonstrating a low recombination probability. That was ascribed to better adhesion of dye 2's molecules on the surface of the TiO<sub>2</sub> with P3HT accompanied by dye 2's atoms easily penetrating through small pinholes distributed on the top of the nc-TiO<sub>2</sub>'s surface. These observations resulted from the difference in the molecular weights of dyes 2 and 3. Using basic calculation methods, dye 2 had a lower molecular weight of 345g/mole that played a role in producing high power efficiency solar cells. Conversely, dye 3's molecular weight was 425g/mole, which exhibited high aggregation on the top of the nc-TiO<sub>2</sub> and did not easily penetrate the pinholes like dye 2's solar cells and produced low-efficiency dye 3 solar cells. Dye 1's solar cells hardly behaved like diodes in the dark,

with a small rectification and onset voltage. Therefore, interfacial layers were created between the P3HT and nc-TiO<sub>2</sub> that could not overcome the charge leakage and did not have enough energy to separate excitons. Dye 1 structure had two groups of cyanoacrylic acids connected to the terthiophene moiety. That caused an increase in the energy gaps between the lowest unoccupied molecular orbital (LUMO) and HOMO, suppressing the HOMO energy level far below the P3HT layer's energy level and increasing the energy level of dye 1 excited state above the TiO<sub>2</sub>'s conduction band. Dye 1 has high molecular weight caused aggregation layers between the nc-TiO<sub>2</sub> and P3HT because the dye had difficulty spreading through the pinholes on the nc-TiO<sub>2</sub> film. That also affected the light absorption and produced a low light current density. According to the equivalent circuit shown in Fig. 10, the shunt resistance was low and produced a small open-circuit voltage with a low onset voltage.

#### 4. Conclusion

To date, considerable research has been devoted to synthesizing new materials for use in organic/inorganic solar cells. The dyes' materials are considered one of the most important components of three-layer solar cells. In this study, three different dyes were synthesized and inserted between the holes and electron transport layers. Dye 2's solar cells had the best high power conversion efficiency and short current density compared with the other dyes. It also suppressed the dark current more than other devices, behaving like diodes with high rectification in the dark. That was attributed to the difference in their molecular structures, which affected the interfacial areas' properties at the junctions.

#### Acknowledgment

The authors wish to thank the Scientific Research Support Fund in Jordan under the program SRF 2010/07/01.

#### Compliance with ethical standards

#### Conflict of interest

The author(s) declared no potential conflicts of interest with respect to the research, authorship, and/or publication of this article.

#### References

Al-Dmour H (2014). Effect of ambient air condition on low frequency negative capacitance of nc-TiO<sub>2</sub>/P3HT heterojunction solar cells. American Journal of Applied Science,

11(8): 1351-1356.

<https://doi.org/10.3844/ajassp.2014.1351.1356>

- Baxter J (2012). Commercialization of dye sensitized solar cells: Present status and future research needs to improve efficiency, stability, and manufacturing. Journal of Vacuum Science and Technology A, 30(2): 020801.  
<https://doi.org/10.1116/1.3676433>
- Burschka J, Pellet N, Moon SJ, Humphry-Baker R, Gao P, Nazeeruddin MK, and Grätzel M (2013). Sequential deposition as a route to high-performance perovskite-sensitized solar cells. Nature, 499(7458): 316-319.  
<https://doi.org/10.1038/nature12340> PMID:23842493
- Hagfeldt A, Boschloo G, Sun L, Lars K, and Pettersson H (2010). Dye-sensitized solar cells. Chemical Reviews, 110(11): 6595-6663. <https://doi.org/10.1021/cr900356p> PMID:20831177
- Knoevenagel E (1894). Ueber eine darstellungsweise der glutarsäure. Berichte der Deutschen Chemischen Gesellschaft, 27(2): 2345-2346.  
<https://doi.org/10.1002/cber.189402702229>
- Li N, Lassiter BE, Lunt RR, Wei G, and Forrest SR (2009). Open circuit voltage enhancement due to reduced dark current in small molecule photovoltaic cells. Applied Physics Letters, 94(2): 13. <https://doi.org/10.1063/1.3072807>
- Nazeeruddin MK, Kay A, Rodicio I, Humphry-Baker R, Müller E, Liska P, and Grätzel M (1993). Conversion of light to electricity by cis-X<sub>2</sub>bis (2, 2'-bipyridyl-4, 4'-dicarboxylate) ruthenium (II) charge-transfer sensitizers (X= Cl-, Br-, I-, CN-, and SCN-) on nanocrystalline titanium dioxide electrodes. Journal of the American Chemical Society, 115(14): 6382-6390. <https://doi.org/10.1021/ja00067a063>
- O'regan B and Grätzel M (1991). A low-cost, high-efficiency solar cell based on dye-sensitized colloidal TiO<sub>2</sub> films. Nature, 353(6346): 737-740. <https://doi.org/10.1038/353737a0>
- Saleh NI, Al-Trawneh S, Al-Dmour H, Al-Taweel S, and Graham JP (2015). Effect of molecular-level insulation on the performance of a dye-sensitized solar cell: Fluorescence studies in solid state. Journal of Fluorescence, 25(1): 59-68.  
<https://doi.org/10.1007/s10895-014-1479-8> PMID:25398318
- Selopal GS, Wu HP, Lu J, Chang YC, Wang M, Vomiero A, and Diau EWG (2016). Metal-free organic dyes for TiO<sub>2</sub> and ZnO dye-sensitized solar cells. Scientific Reports, 6: 18756.  
<https://doi.org/10.1038/srep18756> PMID:26738698 PMCID:PMC4704050
- Stille JK (1986). The palladium-catalyzed cross-coupling reactions of organotin reagents with organic electrophiles [new synthetic methods (58)]. Angewandte Chemie International Edition in English, 25(6): 508-524.  
<https://doi.org/10.1002/anie.198605081>
- Tamao K, Kodama S, Nakajima I, Kumada M, Minato A, and Suzuki AK (1982). Nickel-phosphine complex-catalyzed Grignard coupling—II: Grignard coupling of heterocyclic compounds. Tetrahedron, 38(22): 3347-3354.  
[https://doi.org/10.1016/0040-4020\(82\)80117-8](https://doi.org/10.1016/0040-4020(82)80117-8)
- Wang R, Nakar R, Jiang Y, Berton N, Wu S, Wang Q, and Gao J (2020). Fluorinated interfacial layers in perovskite solar cells: Efficient enhancement of the fill factor. Journal of Materials Chemistry A, 8(32): 16527-16533.  
<https://doi.org/10.1039/D0TA05033D>
- Yella A, Lee HW, Tsao HN, Yi C, Chandiran AK, Nazeeruddin MK, and Grätzel M (2011). Porphyrin-sensitized solar cells with cobalt (II/III)-based redox electrolyte exceed 12 percent efficiency. Science, 334(6056): 629-634.  
<https://doi.org/10.1126/science.1209688> PMID:22053043